



**HAL**  
open science

## Excitation of waves at $2\omega_p$ and back propagating waves at $\omega_p$ : a parametric study

P. Trávníček, P. Hellinger, D. Schriver, M. G. G. T. Taylor

### ► To cite this version:

P. Trávníček, P. Hellinger, D. Schriver, M. G. G. T. Taylor. Excitation of waves at  $2\omega_p$  and back propagating waves at  $\omega_p$ : a parametric study. *Nonlinear Processes in Geophysics*, 2003, 10 (4/5), pp.345-349. hal-00302223

**HAL Id: hal-00302223**

**<https://hal.science/hal-00302223>**

Submitted on 18 Jun 2008

**HAL** is a multi-disciplinary open access archive for the deposit and dissemination of scientific research documents, whether they are published or not. The documents may come from teaching and research institutions in France or abroad, or from public or private research centers.

L'archive ouverte pluridisciplinaire **HAL**, est destinée au dépôt et à la diffusion de documents scientifiques de niveau recherche, publiés ou non, émanant des établissements d'enseignement et de recherche français ou étrangers, des laboratoires publics ou privés.

# Excitation of waves at $2\omega_{p,e}$ and back propagating waves at $\omega_{p,e}$ : a parametric study

P. Trávníček<sup>1</sup>, P. Hellinger<sup>1</sup>, D. Schriver<sup>2</sup>, and M. G. G. T. Taylor<sup>3</sup>

<sup>1</sup>Institute of Atmospheric Physics, Czech Academy of Sciences, Boční II. čp. 1401, 14131 Prague 4, Czech Republic

<sup>2</sup>Institute of Geophysics and Planetary Physics, University of California Los Angeles, Los Angeles, 90095-1567, USA

<sup>3</sup>Mullard Space Science Laboratory, UCL, Holmbury St. Mary, Dorking, Surrey, RH5 6NT, UK

Received: 2 July 2002 – Revised: 2 October 2002 – Accepted: 9 October 2002

**Abstract.** We present a parametric study of electrostatic waves generated with angular frequencies  $2\omega_{p,e}$  and  $-\omega_{p,e}$  by an electron beam using a one-dimensional Vlasov code. We consider a background plasma consisting of three components: two electron populations (a background and a beam) and a proton population (with a mass ratio  $m_p/m_e = 400$  and temperatures  $T_p = T_e = T$ ). We investigate the influence of different beam parameters on the nonlinear growth rate of waves with angular frequency  $2\omega_{p,e}$  and compare the results of the numerical experiments to theoretical predictions. We also examine the presence and excitation of back propagating waves with angular frequency  $\omega_{p,e}$ . A discussion on the possible generating mechanisms of the different modes observed in these simulations is also presented.

## 1 Introduction

The excitation of waves by an electron beam injected into a collisionless plasma has been the subject of several theoretical and numerical studies. Electron beams are a natural source of electrostatic Langmuir waves at the plasma fundamental frequency  $f_{p,e}$ . However, waves at  $2f_{p,e}$  are often observed in the vicinity of the terrestrial electron foreshock region (e.g. Kasaba et al., 2001); these  $2f_{p,e}$  emissions are electromagnetic in nature, whose origin and generating mechanism are not yet well understood. These electromagnetic waves could be connected with the nonlinear electrostatic waves at  $2f_{p,e}$ , usually observed in numerical simulations of plasma-electron beam systems. Electrostatic harmonics of the plasma fundamental frequency have been observed at the very beginning of numerical studies (Klimas, 1983). Recently, Yoon (2000) has published a self-consistent theoretical work on weak turbulence, assuming higher order terms in the perturbation expansion of the Vlasov-Poisson system of equations. Yoon's theory predicts the existence of a nonlinear electrostatic mode, with a growth rate depending

on the energy of the Langmuir waves and on the properties of the electron distribution function. The electromagnetic  $2f_{p,e}$  waves could be the result of a mode conversion from purely electrostatic waves (Yoon et al., 1994).

On the other hand, Kasaba et al. (2001) have shown, using two dimensional particle in cell (PIC) simulations, that Langmuir waves interact with back propagating (with respect to the electron beam) Langmuir waves (Ginzburg and Zheleznyakov, 1958; Dum, 1990). Their interaction naturally generates electromagnetic waves at about  $2f_{p,e}$  (Cairns and Melrose, 1985).

The back propagating mode with angular frequency  $\omega_{p,e}$  (hence forth we denote this mode  $-\omega_{p,e}$ ) has been discussed by (Tsytoich, 1970), and later, for example, by Dum (1990). Dum (1990) examined the appearance of back propagating Langmuir waves in a numerical model containing a mobile proton species. This work noted that waves scattering off ions are much more efficient than waves scattering off of electrons.

In this paper we obtain a quantitative description of the generation of  $2\omega_{p,e}$  and  $-\omega_{p,e}$  electrostatic waves using a set of Vlasov simulations. The two modes have different properties and generating mechanisms, and, therefore, it is likely that their amplitudes vary differently with plasma parameters. We consider a background plasma consisting of two species: an electron population and a proton population, with an artificial mass ratio  $m_p/m_e = 400$ , and we assume equal temperatures of the proton and electron distribution functions,  $T_p = T_e = T$ . The third component present in our model is an electron beam with variable initial parameters. We compare the results of our numerical experiments for  $2\omega_{p,e}$  waves with the theoretical predictions of Yoon's theory (Yoon, 2000; Ziebell et al., 2001; Gaelzer et al., 2002). In addition, we briefly discuss the growth rate of  $-\omega_{p,e}$  waves.

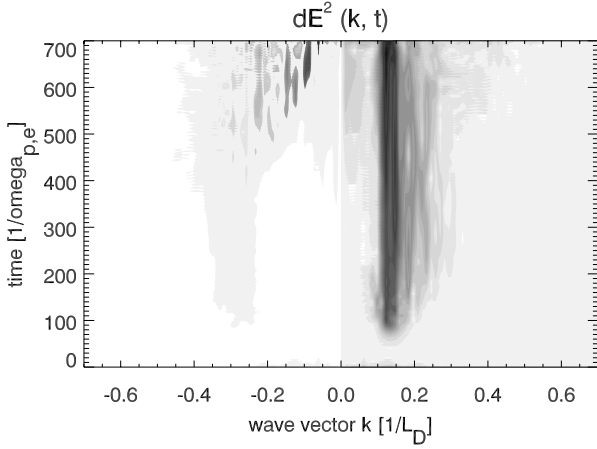


**Fig. 1.** Figure shows a typical evolution of the fluctuating wave energy  $|\delta E^2(k, t)|$  for  $t \in (0, 700) \omega_{p,e}^{-1}$  as a gray scale plot. The data shown corresponds to the case with parameters:  $v_b = 8.7 v_{e,th}$ ,  $n_b = 0.03 n$ ,  $T_b = 2.3 T$ .

## 2 The numerical model

In order to simulate the interaction of an electron beam and a plasma we use the second order numerical scheme for the Vlasov-Poisson system of equations:

$$\left( \frac{\partial}{\partial t} + \mathbf{v} \cdot \nabla + \frac{e_a}{m_a} \mathbf{E}(\mathbf{r}, t) \cdot \frac{\partial}{\partial \mathbf{v}} \right) f_a(\mathbf{r}, \mathbf{v}, t) = 0, \quad (1)$$

$$\nabla \cdot \mathbf{E}(\mathbf{r}, t) = \frac{n}{\epsilon_0} \sum_a e_a \int d\mathbf{v} f_a(\mathbf{r}, \mathbf{v}, t),$$

where  $f_a$  denotes the distribution function of a given species  $a$  ( $a = e$  for electrons,  $a = p$  for protons), defined in two dimensional phase space  $\mathcal{S} = \mathcal{S}(x, v_x)$ .  $n = \bar{n}_e = \bar{n}_p$  denotes the ambient plasma density, and  $\mathbf{E}$  represents the self-consistent electrostatic field. We use a standard numerical scheme to resolve the Vlasov-Poisson system: For the integration of the Poisson equation we use a finite difference scheme, the time advance scheme of the Vlasov equation is based on a splitting algorithm first introduced by Cheng and Knorr (1976) and an upwind discretisation (Leer, 1977), later extended by Fijalkow (1999). Our code is based on a slightly modified numerical scheme described by Fijalkow (1999).

We use the Debye length  $\lambda_D$  (denoted by  $L_D$  on figures) as the unit of space and the inverse of the plasma angular frequency  $\omega_{p,e}^{-1}$  as the unit of time. The length,  $L_x$ , of the spatial domain equals  $512 \lambda_D$ , sampled over  $n_x = 1024$  points, i.e.  $dx = 0.5 \lambda_D$ . The size and sampling of the velocity domain for the electrons and protons is given by the parameters  $|v_{e,min}| = |v_{e,max}| = 22 v_{e,th}$ , ( $dv_e = 0.147 v_{e,th}$ ), and  $|v_{p,min}| = |v_{p,max}| = 12 v_{p,th}$ , ( $dv_p = 0.12 v_{p,th}$ ) respectively. Here  $v_{a,th}$ , represents the thermal speed of the electrons ( $a = e$ ) and protons ( $a = p$ ).

We use periodic boundary conditions for the distribution function and the electric field in the spatial domain and cut off values  $v_{a,min}$ ,  $v_{a,max}$  for distribution functions in the velocity domain.

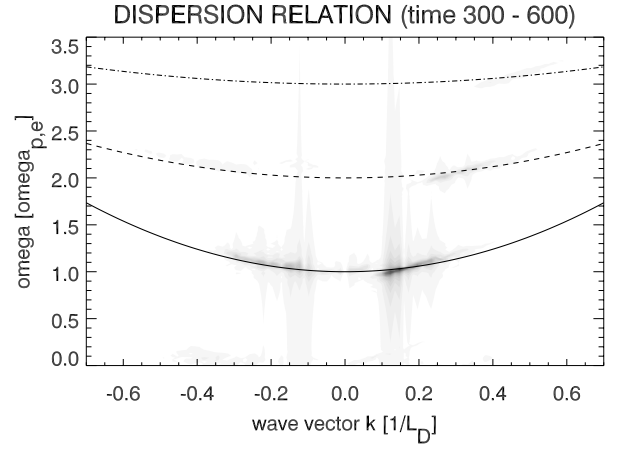


**Fig. 2.** Simulated spectrum of the fluctuating wave energy  $\delta E^2$  as a function of angular frequency  $\omega$  and wave vector  $k$  calculated during the interval  $\Delta t = 300 - 600 \omega_{p,e}^{-1}$ . The solid curve shows the linear dispersion relation  $\omega_{\mathbf{k},1} = \omega_{p,e} (1 + 3/2 k^2 \lambda_D^2)$ , the dashed curve shows the nonlinear dispersion relation  $\omega_{\mathbf{k},2} = \omega_{p,e} (2 + 3/4 k^2 \lambda_D^2)$ , and the dot-dashed curve shows the expected theoretical nonlinear dispersion relation  $\omega_{\mathbf{k},3} = \omega_{p,e} (3 + 3/8 k^2 \lambda_D^2)$ .

## 3 The parametric study

We examine the nonlinear properties of the beam-plasma interaction, specifically the generation of  $2 \omega_{p,e}$  and  $-\omega_{p,e}$  waves, for different electron beam parameters. We consider a plasma consisting of three components: background electrons, protons, and an electron beam. The temperature of the background electrons and protons are equal to each other,  $T_e = T_p = T$ . We perform 30 numerical experiments with varying beam parameters: Beam density ( $n_b = 0.015 n$  and  $n_b = 0.03 n$ ), velocity with respect to the background electrons ( $v_b = 8.1, 8.4, 8.7, 9.0 v_{e,th}$ ), and temperature ( $T_b = 2.0, 2.3, 2.8 T$ ).

All the simulations have similar properties, the electron beam generates Langmuir waves and the instability saturates later on. During the nonlinear evolution,  $2 \omega_{p,e}$  and  $-\omega_{p,e}$  waves appear. Figure 1 shows a typical evolution of simulated wave spectra of fluctuating wave energy  $|\delta E^2(k, t)|$  as a gray scale plot with parameter values:  $v_b = 8.7 v_{e,th}$ ,  $n_b = 0.03 n$ ,  $T_b = 2.3 T$ , where  $E(k, t)$  is obtained by a fourier transform of the electric field  $E(x, t)$  in space. The figure illustrates the growth of the beam-generated Langmuir waves  $\omega_{p,e}$  with  $k \sim 0.1 - 0.2/\lambda_D$ , later on the  $2\omega_{p,e}$  waves with  $k \sim 0.3/\lambda_D$ , and finally the growth of  $-\omega_{p,e}$  waves with  $k \sim -0.1 - 0.2/\lambda_D$ . The dispersion relation from our numerical model for the same simulation is shown in Fig. 2. Figure 2 displays the simulated spectrum  $|\delta E^2(k, \omega)|$  calculated for the period  $300 - 600 \omega_{p,e}^{-1}$ . The solid line on the plot corresponds to the theoretical fundamental plasma frequency  $\omega_{\mathbf{k},1}$ ,

$$\omega_{\mathbf{k},1} = \omega_{p,e} \left( 1 + \frac{3}{2} k^2 \lambda_D^2 \right), \quad (2)$$

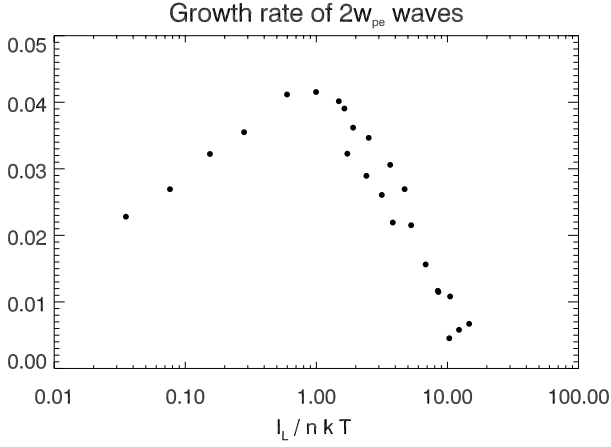


**Fig. 3.** Approximate growth rate of  $2\omega_{p,e}$  waves for different simulations as a function of the corresponding Langmuir waves amplitude,  $I_L / n k T$ .

the dashed line corresponds to the theoretical frequency  $\omega_{\mathbf{k},2}$  as derived by Yoon (2000) and in agreement with Kasaba et al. (2001):

$$\omega_{\mathbf{k},2} = \omega_{p,e} \left( 2 + \frac{3}{4} k^2 \lambda_D^2 + \varepsilon_{\mathbf{k}} \right), \quad (3)$$

where we assume that the thermal corrections are negligible,  $\varepsilon_{\mathbf{k}} \approx 0$  and finally, the dot-dashed line corresponds to a fit suggesting the theoretical frequency  $\omega_{\mathbf{k},3}$  to be:

$$\omega_{\mathbf{k},3} = \omega_{p,e} \left( 3 + \frac{3}{8} k^2 \lambda_D^2 \right). \quad (4)$$

Note that Eq. (3) has been derived as an approximate solution of the non-linear eigenmode analysis retaining the non-linear wave coupling term which arises from the presence of a broad spectrum of incoherent Langmuir waves (Gaelzer et al., 2002; Yoon, 2000).

The numerical simulations carried out in this paper show that the main parameter that governs the plasma properties is the time averaged energy  $I_L$

$$I_L = \int_{\Delta\omega} \int_{\Delta k} \delta E^2(k, \omega) d\omega dk \quad (5)$$

of the beam-generated Langmuir waves. Each energy spectra  $|\delta E^2(\omega, k)|$  considered in this paper was calculated over the time interval of duration  $\Delta t = 300 \omega_{p,e}^{-1}$ .

All modes at  $\omega_{p,e}$ ,  $2\omega_{p,e}$ ,  $3\omega_{p,e}$ , and weak  $-\omega_{p,e}$ , are well defined in Fig. 2. The theoretical curves (2), (3) and (4) do not take into account the presence of electron beam on the dispersion of the modes. This fact explains the small difference between the theoretical prediction (2) and the spectrum of Langmuir waves observed in the simulations (Ciarins, 1989). The discrepancy between the harmonic emission and the corresponding dispersion curve (3) could possibly be attributed to the same effect. Figure 3 shows an approximate growth rate of  $2\omega_{p,e}$  waves for different simulations,

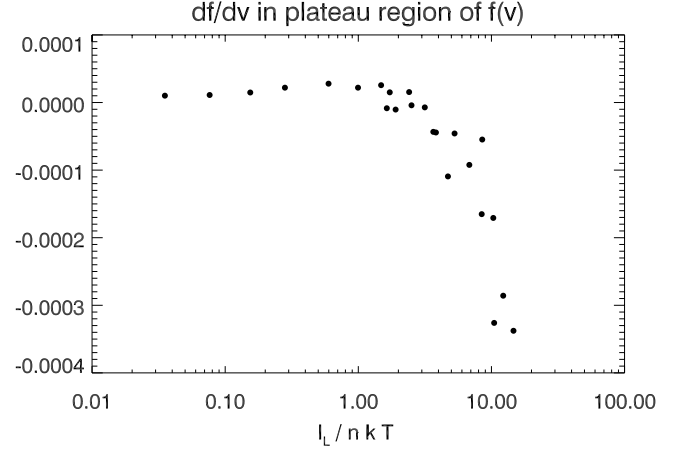


**Fig. 4.** The derivative  $\partial f / \partial v$  calculated in the plateau region of  $f(v)$  for different simulations as a function of the corresponding Langmuir wave amplitude,  $I_L / n k T$ .

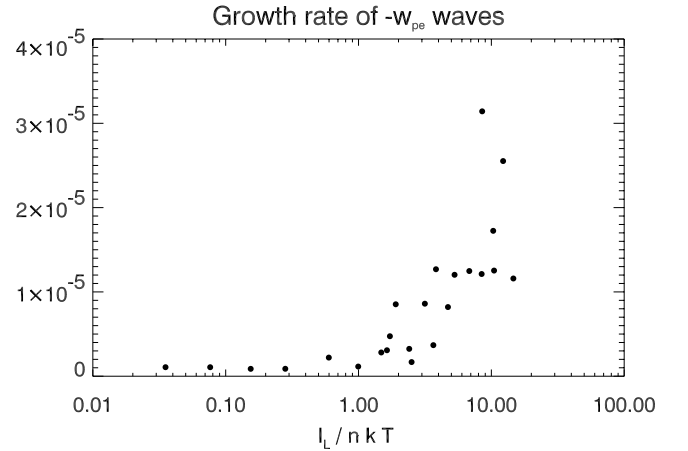


**Fig. 5.** An estimation of the growth rate of  $-\omega_{p,e}$  waves for different simulations as a function of the corresponding Langmuir waves amplitude,  $I_L / n k T$ .

as a function of the corresponding amplitude of the Langmuir waves  $I_L / n k T$ : its growth rate increases with  $I_L / n k T$  for  $I_L / n k T < 1$  and decreases for  $I_L / n k T > 1$ . This change in behaviour is connected to the change of character of the electron distribution function in the nonlinear stage, which can be seen in Fig. 4. Figure 4 shows the derivative  $\partial f / \partial v$ , calculated in the plateau region ( $v \sim 6 - 8v_{e,th}$ , see Fig. 6) of the electron distribution function  $f_e(v)$  for different simulations, as a function of the corresponding amplitude of the Langmuir waves  $I_L / n k T$ . Figure 4 clearly shows that the plateau in the electron distribution function is not formed when  $I_L / n k T > 1$ , since in this region  $\partial f / \partial v < 0$ .

An estimate of the growth rate of backward propagating waves at  $\omega_{p,e}$  is shown in Fig. 5. Figure 5 displays the growth rate of  $-\omega_{p,e}$  waves for different simulations, as a function of the corresponding amplitude of the Langmuir waves  $I_L / n k T$ . The growth rate of these waves increases under

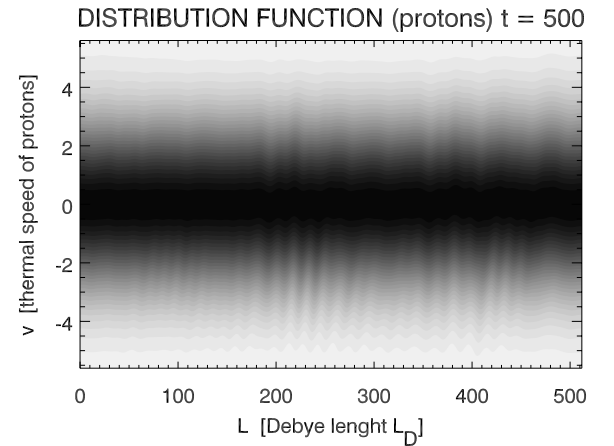
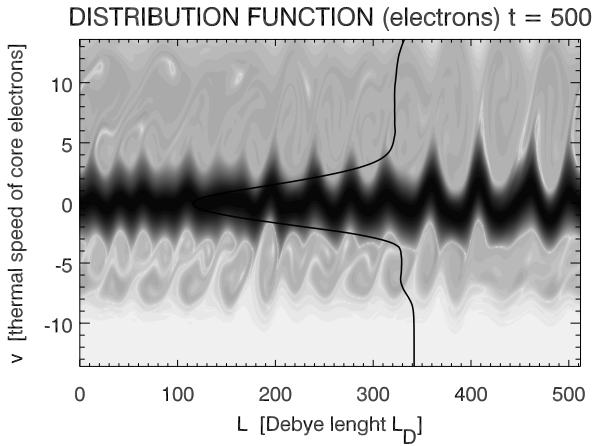
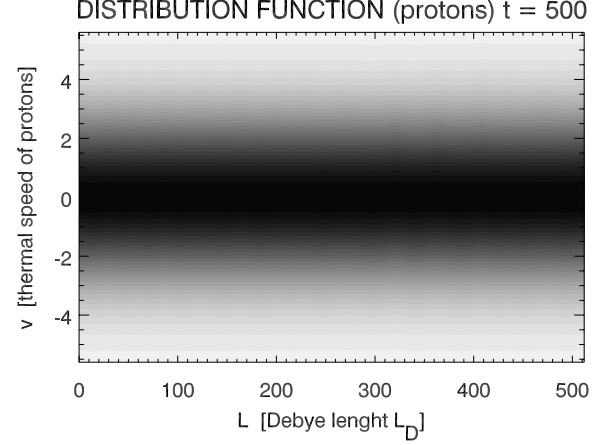
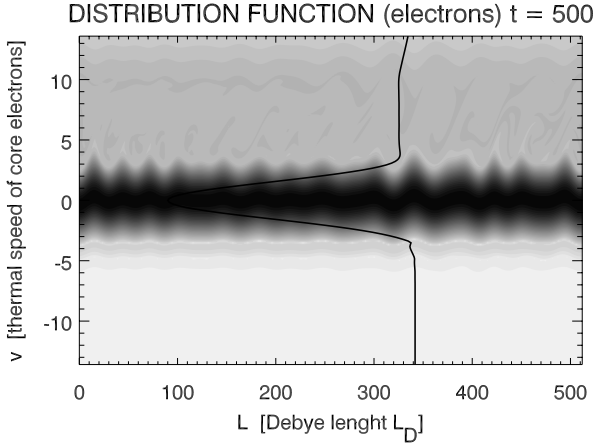


**Fig. 6.** The electron distribution function in the nonlinear stage of the simulation ( $t = 500 \omega_{p,e}^{-1}$ ). The upper panel corresponds to the case with  $n_b = 0.015 n$ ,  $v_b = 8.1 v_{e,th}$ ,  $T_b = 2.8 T_e$ , and  $I_L / n_e k T_e \sim 0.02$ . The lower panel shows the case with  $n_b = 0.03 n_e$ ,  $v_{b,x} = 9.0 v_{e,th}$ ,  $T_b = 2.0 T_e$ , and  $I_L / n_e k T_e \sim 16$ . Solid curves show a profile of the corresponding distribution function averaged over  $x$ .

**Fig. 7.** The proton distribution function in the nonlinear stage of the simulation ( $t = 500 \omega_{p,e}^{-1}$ ). The upper panel corresponds to the case with  $n_b = 0.015 n$ ,  $v_b = 8.1 v_{e,th}$ ,  $T_b = 2.8 T_e$ , and  $I_L / n_e k T_e \sim 0.02$ . The lower panel shows the case with  $n_b = 0.03 n_e$ ,  $v_{b,x} = 9.0 v_{e,th}$ ,  $T_b = 2.0 T_e$ , and  $I_L / n_e k T_e \sim 16$ .

the influence of stronger turbulence  $I_L / n k T > 1$ .

The results show that the output of the simulation is different for  $I_L / n k T < 1$  and  $I_L / n k T > 1$ , which can be seen in particular for the electrons and protons in the nonlinear stage. Figures 6 and 7 show the distribution function  $f(x, v)$  of the electrons and protons respectively, in the nonlinear stage. Figure 6 also shows a profile (solid curve) of the distribution function  $f(v)$ , the average value of  $f(x, v)$  over  $x$ .

The left panels of Figs. 6 and 7 correspond to the case with  $n_b = 0.015 n$ ,  $v_b = 8.1 v_{e,th}$ ,  $T_b = 2.8 T_e$ , and  $I_L / n_e k T_e \sim 0.02$  (the weakest Langmuir turbulence from our simulation set). The right panels show the case with  $n_b = 0.03 n_e$ ,  $v_{b,x} = 9.0 v_{e,th}$ ,  $T_b = 2.0 T_e$ , and  $I_L / n_e k T_e \sim 16$  (the strongest Langmuir turbulence from our simulation set).

Figure 6 shows signatures of vortices, indicating electron trapping. These vortices are thermalized in the latter stages

of the simulation (cf. Kasaba et al., 2001) for the case of weak turbulence. Figure 6 (right panel) also shows the impact of backscattered Langmuir waves on the electron distribution function: with the formation of a plateau for negative velocities (cf. Ziebell et al., 2001).

#### 4 Concluding remarks

This study gives a quantitative description of the threshold between weak and strong turbulence cases, based on the theoretical approach developed by Yoon (2000). We have performed 30 numerical experiments using a standard numerical model for the Vlasov-Poisson system.

Generalized weak turbulence theory by Yoon (2000) predicts the existence of a nonlinear mode around  $2 \omega_{p,e}$ , unstable for strong enough Langmuir turbulence, with a growth rate  $\gamma_2 \omega_{p,e}$  proportional to the amplitude of the Langmuir wave. Figure 3 shows that when the energy of the Langmuir waves  $I_L$  exceeds the thermal energy of the background elec-

trons  $n_e k T_e$ , the growth rate  $\gamma_{2\omega_{p,e}}$  decreases with  $I_L$ . We can consider the point  $I_L / n_e k T_e = 1$  as a characteristic endpoint of the weak turbulence. Our simulations show qualitatively similar results to those of Ziebell et al. (2001) and Gaelzer et al. (2002) who studied a weak beam-plasma instability solving numerically the equations of (generalized) weak plasma turbulence kinetic theory. Further comparisons of Vlasov simulations and the work of Ziebell et al. (2001) and Gaelzer et al. (2002) requires the use of comparable plasma parameters and is out of the scope of this paper.

The simulation set shows that under the condition of strong Langmuir turbulence, the electrons tend to decelerate and move closer to the background distribution function (the derivative  $\partial f / \partial v_x$  calculated in the plateau region is negative). So the derivative  $\partial f / \partial v_x$  is a parameter connected with the ratio  $I_L / n_e k T_e$  describing the strength of the Langmuir turbulence. We can conclude that the generalized weak turbulence theory (Yoon, 2000) is valid when the amplitude of the primary Langmuir waves satisfies the relation

$$\frac{I_L}{n_e k T_e} < 1. \quad (6)$$

Further analysis should be made to check whether the parameter  $\partial f / \partial v_x$  plays a compensating role in the plasma for  $I_L / n_e k T_e > 1$ , so that Yoon's theory of generalized weak turbulence is also valid when the energy in the Langmuir waves  $I_L$  exceeds the thermal energy of background electrons (see Fig. 4).

The time duration of the simulations has not been sufficient to investigate the  $-\omega_{p,e}$  mode more closely. Figure 5 indicates a slight increase in the growth rate of this mode once the plasma becomes more turbulent and the backscattering of waves off ions is more likely (see Fig. 7), although the rates are too small to make any solid conclusions. This result is in agreement with Dum (1990), who concluded that these waves are generated by the backscattering of electrons from thermal fluctuations of the proton distribution function. To study this phenomena more closely will require further numerical experiments using the later nonlinear stage of the current model.

*Acknowledgement.* We acknowledge the support of grants GAAV B3042106 and ESA PRODEX 14529/00/NL/SFe.

## References

- Cairns, I. H.: Electrostatic wave generation above and below the plasma frequency by electron-beams, *Phys. Fluids B.*, 1, 204–213, 1989.
- Cairns, I. H. and Melrose, D. B.: A theory for the  $2 f_p$  radiation upstream of the Earth's shock, *J. Geophys. Res.*, 90, 6637–6640, 1985.
- The integration of the Vlasov equation in configuration space, *J. Comp. Phys.*, 22, 330–351, 1976.
- Dum, C. T.: Simulation studies of plasma waves in the electron foreshock: The generation of langmuir waves by a gentle bump-on-tail electron distribution, *J. Geophys. Res.*, 95, 8095–8110, 1990.
- Fijalkow, E.: Numerical solution to the Vlasov equation: The 1D code, *Comp., Phys. Comm.*, 116, 329–335, 1999.
- Gaelzer, R.; Zeibell, L. F., and Yoon, P. H.: Generation of harmonic langmuir mode by beam-plasma instability, *Phys. of Plasmas*, 8, 96–110, 2002.
- Ginzburg, V. L. and Zheleznyakov, V. V.: On the possible mechanisms of sporadic solar radio emission (radiation in an isotropic plasma), *Sov. Phys. Astron.*, 2, 653, 1958.
- Kasaba, Y., Matsumoto, H., and Omura, Y.: One- and two-dimensional simulations of electron beam instability: Generation of electrostatic and electromagnetic  $2 f_p$  waves, *J. Geophys. Res.*, 106, 18 693–18 711, 2001.
- Klimas, A. J.: A mechanism for plasma waves at the harmonics of the plasma frequency in the electron foreshock boundary, *J. Geophys. Res.*, 88, 9081–9091, 1983.
- Leer, B. V.: Towards the ultimate conservative difference scheme: Iv. a new approach to numerical convection, *J. Comp. Phys.*, 23, 263, 1977.
- Tsytovich, V. N.: *Nonlinear effects in a plasma*, Plenum, New York, 1970.
- Yoon, P. H.: Generalized weak turbulence theory, *Phys. of Plasmas*, 7, 4858–4970, 2000.
- Yoon, P. H., Wu, C. S., Vinas, A. F., Reiner, M. J., Fainberg, J., and Stone, R. G.: Theory of  $2\omega_{p,e}$  radiation induced by the bow shock, *J. Geophys. Res.*, 99, 23 481–23 488, 1994.
- Ziebell, L. F., Gaelzer, R., and Yoon, P. H.: Nonlinear development of weak beam-plasma instability, *Phys. of Plasmas*, 8, 3982–3995, 2001.